Quantum calculation of vibrational states in the aniline–argon van der Waals cluster

P. Parneix, N. Halberstadt, and Ph. Bréchignac
Laboratoire de Photophysique Moléculaire, C.N.R.S, Université de Paris-Sud, Bâtiment 213, F-91405 Orsay Cedex, France

F. G. Amar
Department of Chemistry, University of Maine, Orono, Maine 04469

A. van der Avoird and J. W. I. van Bladel
Institute of Theoretical Chemistry, University of Nijmegen, Toernooiveld, 6525 ED Nijmegen, The Netherlands

(Received 27 August 1992; accepted 2 November 1992)

Theoretical calculations of vibrational intermolecular states of the aniline–argon van der Waals complex for $J=0$ are reported. A fully-quantum method (LCHOP) was used in order to describe the van der Waals cluster. Results in the first two electronic states S_0 ($\tilde{X}\,^1A_1$) and S_1 ($\tilde{A}\,^1B_2$) are presented; in the S_1 state a comparison with available experimental data is made. We introduce an additive repulsive interaction between N and Ar in the S_1 state in order to account for the spectral features observed in larger clusters. Several parametrizations of this term in the potential are discussed with a view to applications to semiclassical simulation of the spectra of the larger An–Ar_n clusters.

I. INTRODUCTION

During the last decade, many workers have been interested in the study of van der Waals (vdW) clusters consisting of an aromatic molecule embedded in a cluster of polarizable atoms (or molecules).[1–11] These van der Waals clusters represent a very interesting class of systems for studying the evolution of chemical and physical properties as a function of the size of the cluster or as a function of the solvent properties. One of the ultimate goals of these studies is the understanding of the solvation process. Moreover, clusters provide an ideal means to investigate the evolution of atomic or molecular properties from the isolated species to the bulk.

The influence of the solvent on the spectroscopic properties of the chromophore has been extensively studied. The most important results concern the shift of the first electronic transition[1–11] and of the ionization potential.[12–14] Although the existence of isomers for clusters of a given size has long been postulated, the assignment of spectral bands to specific isomers has been done only recently.[4,10,11] High resolution spectroscopy can be used in order to determine the structures of these isomers.[15–20]

The dynamical behaviour of these weakly bound systems also represents an interesting field of investigation. The coupling between intramolecular and intermolecular modes[21,22] and the predissociation processes[23–26] have been substantially explored. In this case the main goal is the understanding of the redistribution of vibrational energy in such weakly bound systems. More generally, it provides a stringent test for multidimensional van der Waals potentials. Quantum mechanical 3D calculations of bound states in clusters involving aromatic molecules are not many: they are limited to the case of one argon atom bound to benzene,[27] fluorene[27,28] and tetrazine.[29]

In this work, we describe the aniline-argon cluster by a fully quantum mechanical approach. One of the goals of this work is to check the assignments of spectral bands proposed in a previous paper.[10] More generally, we are interested in the construction of an effective potential in the first electronic state in order to reproduce both the experimental blue-shifts of the electronic transition in bigger clusters An–$(Ar)_n$ ($n>1$) and the set of van der Waals frequencies observed for $n=1$.

II. THEORY AND NUMERICAL METHODS

The LCHOP (linear combination of harmonic oscillator products) method which is used in this work has been previously introduced and described in detail by Brocks and Van Koeven.[28] Here we present only a summary and explain the main points.

The body-fixed (BF) frame chosen to describe the motions of the aniline–argon complex has its origin at the center-of-mass of this complex. We let the orientation of this frame be determined only by the semirigid aniline molecule and not by the weakly bound argon atom. We achieve this by choosing the axes of the BF frame on the dimer parallel to the axes of an Eckart frame[30] on the aniline molecule. The motions of the complex, apart from the overall translation which is exactly separable, can then be expressed in the following coordinates:

— The three Euler angles that relate the orientations of the BF axes to a laboratory frame.

— The internal coordinates of the semirigid aniline molecule; these are small displacements from an equilibrium structure that can be transformed into normal coordinates $\{Q_l;\ l=1,...,36\}$.

— The Cartesian components $\mathbf{d}=(d_x,d_y,d_z)$ of the vector that points from the aniline center-of-mass to the argon nucleus.

The latter $36+3$ coordinates, which describe the internal motions of the complex, are all defined with respect to

 0021-9606/93/042709-11$06.00

the BF frame. Although we have used only the Eckart conditions of the aniline molecule to fix the orientations of the BF frame, it has been shown by Brocks and Van Koeven[28] that the 39 internal coordinates of the complex also satisfy a set of Eckart conditions for the whole complex. This is easily understood as follows. In the Eckart conditions that fix the orientation of the frame, one needs a reference geometry which is usually chosen as the equilibrium geometry of the system. If one chooses, in this case, a reference geometry of the complex with $\mathbf{d}=\mathbf{0}$, then the position of the argon atom does not occur in the Eckart conditions that fix the orientation of the frame, and the BF frame on the whole complex is parallel to the aniline frame. This does not lead to an optimum separation between the vibrations and the overall rotation of the complex, but for a system such as we have here, with a large nearly rigid molecule and a weakly bound atom, it offers important computational advantages. As our coordinates satisfy the Eckart conditions for the complex, we can describe the overall and internal motions by the kinetic energy operator derived by Watson[31]

$$T=-\frac{\hbar^2}{2\mu}\nabla^2(\mathbf{d})-\frac{\hbar^2}{2}\sum_{l=1}^{36}\frac{\partial^2}{\partial Q_l^2}+\frac{1}{2}\sum_{i,j}\mu_{ij}(J_i+\Pi_i+l_i)\times(J_j+\Pi_j+l_j)-\frac{\hbar^2}{8}\sum_i\mu_{ii}, \quad (1)$$

where $\mu=mM/(m+M)$ is the complex reduced mass (m is the mass of argon and M the mass of aniline), the J_i are the body-fixed components of the total angular space momentum, the l_i are the components of the orbital angular space momentum of the Ar atom,

$$l_i=\frac{\hbar}{i}\left(d_j\frac{\partial}{\partial d_k}-d_k\frac{\partial}{\partial d_j}\right) \quad \text{with } i,j,k \text{ cyclic}$$

and the Π_i are the components of the vibrational angular momentum of the aromatic molecule which depend on the normal coordinates Q_l and their conjugate momenta. Finally, the μ_{ij} are the body-fixed components of the inverse of the moment of inertia tensor of aniline. Note that the μ_{ij} do not depend on $\mathbf{d}$. As long as we do not neglect the rotation-vibration coupling contained in the third term of this Hamiltonian, the choice of $\mathbf{d}=\mathbf{0}$ in the Eckart conditions does not imply any approximation.

The total Hamiltonian of the system is

$$H=T+V(\mathbf{d},\mathbf{Q}), \quad (2)$$

where $V(\mathbf{d},\mathbf{Q})$ is the total potential energy, which can be separated as

$$V(\mathbf{d},\mathbf{Q})=V(\mathbf{Q})+V_{\text{int}}(\mathbf{d},\mathbf{Q}). \quad (3)$$

Here, $V_{\text{int}}(\mathbf{d},\mathbf{Q})$ is the interaction potential between the Ar atom and the molecule that vanishes at infinite separation and $V(\mathbf{Q})$ is the intramolecular potential of the aromatic molecule. Since in the region of interest, $V_{\text{int}}(\mathbf{d},\mathbf{Q})$ is much weaker than $V(\mathbf{Q})$ and, therefore, the Van der Waals vibrations are considerably slower than the intramolecular vibrations of aniline, we can make an adiabatic separation. The fast intramolecular motions are

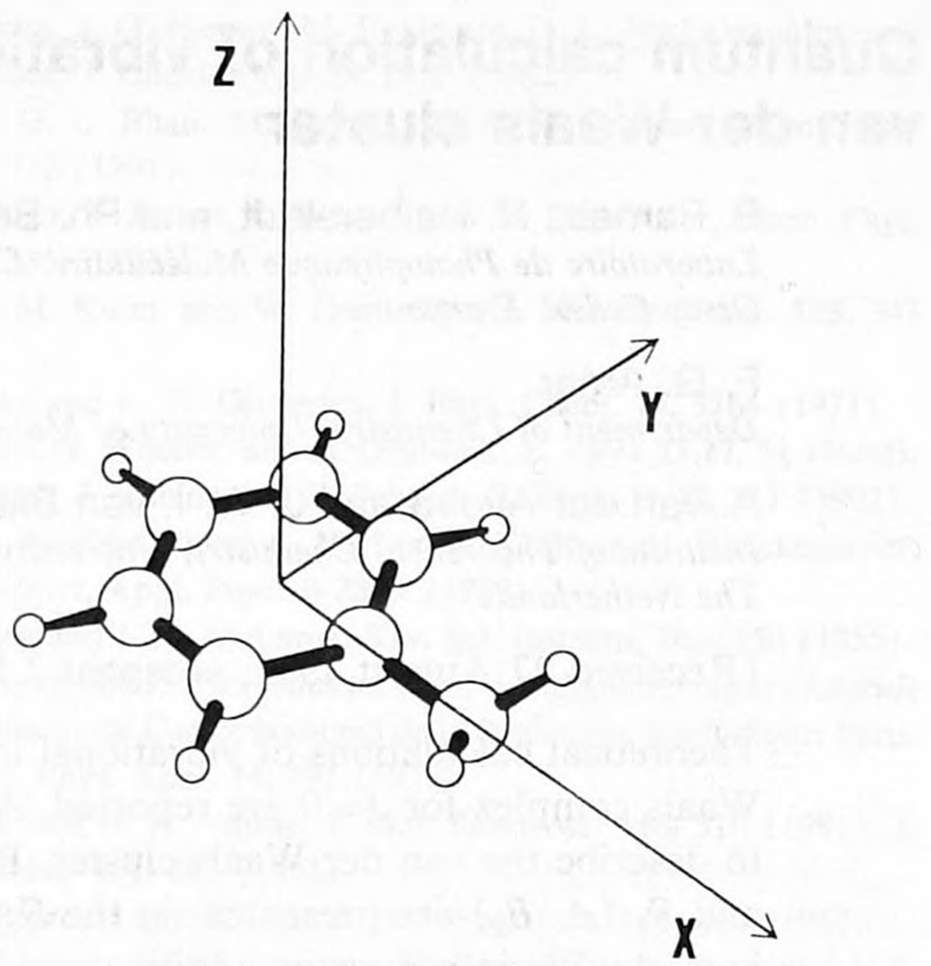

FIG. 1. Sketch of the aniline molecule and the body-fixed frame used throughout this work.

solved first; the corresponding eigenvalues and eigenfunctions Φ_v depend parametrically on the slow coordinates. For a given vibrational state (v) of the aniline molecule, we obtain the following effective Hamiltonian for the van der Waals vibrations and overall rotations of the complex

$$H_{\text{eff}}^{(v)}=-\frac{\hbar^2}{2\mu}\nabla^2(\mathbf{d})+\frac{1}{2}\sum_i I_i^{(v)^{-1}}(J_i+l_i)^2+V_{\text{int}}^{(v)}(\mathbf{d})+\langle U\rangle_v \quad (4)$$

with

$$V_{\text{int}}^{(v)}(\mathbf{d})=\langle\Phi_v|\,V_{\text{int}}(\mathbf{d},\mathbf{Q})\,|\Phi_v\rangle \quad (5)$$

and

$$\langle U\rangle_v=\left\langle\Phi_v\middle|\left(-\frac{\hbar^2}{8}\sum_i\mu_{ii}+\frac{1}{2}\sum_{ij}\mu_{ij}\Pi_i\Pi_j\right)\middle|\Phi_v\right\rangle. \quad (6)$$

In order to obtain Eq. (4), we have chosen the BF axes along the principal inertia axes of the vibrational state of aniline considered, so that the inertia tensor $I^{(v)}$ is diagonal. Only the ground vibrational state is considered in this work and the axes are actually attached to the equilibrium structure, as shown in Fig. 1. The terms linear in Π_i vanish.[28] The term $\langle U\rangle_v$ may be omitted from our calculations, since it is constant for a given intramolecular state. Then, $H_{\text{eff}}^{(v)}$ may be separated into a purely vibrational Hamiltonian

$$H_{\text{vib}}^{(v)}=-\frac{\hbar^2}{2\mu}\nabla^2(d)+\frac{1}{2}\sum_i I_i^{(v)^{-1}}l_i^2+V_{\text{int}}^{(v)}(\mathbf{d}) \quad (7)$$

which is independent of $\mathbf{J}$, and a rovibrational part

$$H_{\text{rovib}}^{(v)}=\frac{1}{2}\sum_i I_i^{(v)^{-1}}J_i^2+\sum_i I_i^{(v)^{-1}}l_iJ_i. \quad (8)$$

We have first calculated the eigenfunctions of $H_{\text{eff}}^{(v)}$ for $\mathbf{J}=\mathbf{0}$, i.e., the eigenfunctions of $H_{\text{vib}}^{(v)}$, and next we have included $H_{\text{rovib}}^{(v)}$ by perturbation theory, as explained in Ref. 28.

The eigenfunctions of $H_{\text{vib}}^{(v)}$ are expanded in a basis of products of harmonic oscillator functions

$$\Phi_n(\mathbf{d})=\sum_{k=0}^{K'}\sum_{l=0}^{L'}\sum_{m=0}^{M'} C_{k,l,m}^{(n)} K_k(d_x) L_l(d_y) M_m(d_z) \tag{9}$$

with

$$K_k(d_x)=N_k \exp(-\tfrac{1}{2}\gamma_x^2 x^2) H_k(\gamma_x x),$$

$$x=d_x-d_x^e,$$

$$\gamma_x=(\mu\omega_x)^{1/2},$$

and analogous expressions for L_l and M_m. The functions H_k are Hermite polynomials, with the normalization factors $N_k=\gamma_x^{1/2}(\pi^{1/2}2^k k!)^{-1/2}$, μ is the reduced mass of the van der Waals complex, as defined in Eq. (1), and ω_x, ω_y, ω_z are harmonic oscillator frequencies. In this case, ω_x, ω_y, and ω_z are variational parameters that may be optimized in order to minimize the number of basis functions required to reach convergence. The harmonic oscillator functions are centered at $\mathbf{d}^e$, which has been taken as the equilibrium position of the Ar atom in the S_0 state.

The matrix elements of the kinetic energy operator in this basis are calculated analytically by expressing this operator in terms of creation and annihilation operators.[32] The matrix elememts of the potential energy operator are computed numerically with a Gauss–Hermite integration.[33] All the results have been obtained with $K'=8$, $L'=8$, $M'=6$, and a grid for numerical integration of 20 points for each coordinate. We have found that $\omega_x=4$ cm^{-1}, $\omega_y=4$ cm^{-1}, $\omega_z=33$ cm^{-1} are suitable values. These frequencies and the components of $\mathbf{d}^e$ (equilibrium position in S_0: -0.08, 0.00, 3.47 Å) are chosen to be the same for the S_0 and S_1 states in order to facilitate the calculation of Franck–Condon factors (see Appendix B).

III. INTERMOLECULAR POTENTIALS

The interaction potential between the aniline molecule and the Ar atom has been constructed as a sum of pairwise atom-atom terms, with an induction term (calculated in the point dipole approximation) added to account for dipole induced-dipole interaction. The values of the permanent dipole of aniline in both S_0 and S_1 electronic states are taken from Lombardi.[34] The parameters for the atom–atom potentials in the S_0 state are taken from Ondrechen *et al.*[35] for the C–Ar and H–Ar interactions and from Bieske *et al.*[11] for N–Ar. Parametrization in the S_1 state has been adjusted in order to reproduce the observed experimental red-shift of 53.2 cm^{-1} [10,11] of the origin of the $S_1\leftarrow S_0$ electronic transition in An–Ar with respect to the corresponding transition in the free molecule. At the end of this section, we will explain how the relevant parameters have been chosen.

Experimental results have also been obtained in our group on the electronic shifts of bigger clusters An–Ar$_n$ ($n=1$, 6).[10] They demonstrate in particular the existence of two isomers for An–Ar$_3$, one of them exhibiting a net blue shift of $+22.5$ cm^{-1} with respect to the bare molecule. Similar results have been obtained by Bieske *et al.*[11] The calculated minimum energy structures (obtained with molecular dynamics simulations associated with the quenching method) for An–Ar$_3$ in the S_0 state, using the same model potential, [10] show that the main stable isomers involve at least one Ar atom interacting strongly with the nitrogen atom in the $-NH_2$ substituent: In the (3/0) conformer (3 atoms on the same side of the plane of the molecule) one Ar atom takes place near the center of the aromatic ring and the other two are located symmetrically on each side of the nitrogen atom while forming, together with the central atom, an argon trimer sitting on the plane of the molecule; in the (2/1) conformer a single Ar atom interacts with the nitrogen in a similar location and the two others occupy opposite central ring positions. In order to explain the spectra we have introduced a modified shift additivity rule[10] which implies the assignments of "site-specific shifts" to different binding sites. This led us to assign a -52 cm^{-1} (red) shift to the "ring" site and a $+35$ cm^{-1} (blue) shift to the "nitrogen" site.

Recently, Meijer *et al.*[20] have observed a similar effect in the triphenylamine (TPA)–Ar cluster. They measured a net blue shift of $+211$ cm^{-1} relative to the free molecule for the $S_1\leftarrow S_0$ transition in this cluster. High resolution spectroscopy performed to determine the structure of this isomer showed that the Ar atom takes place exactly on the C_3 symmetry axis just above the nitrogen atom (the equilibrium distance between N and Ar being equal to 4.0 Å). There is no doubt that the blue shifts for Ar interacting with nitrogen in these molecules is due to a perturbation by the Ar atom of the electronic cloud associated with the nitrogen lone pair electrons.

In order to reproduce this special interaction between argon and nitrogen atoms, we have included an additional term centered on the N atom in the intermolecular surface for the S_1 state. Although it is a positive term which makes it look like a purely repulsive interaction, it is actually describing the reduction of the attraction when the molecule is excited from S_0 to S_1. In this paper, we have used two different parametrizations of this additional term and we will discuss the influence of these two different empirical potentials on the calculated intermolecular frequencies.

These two potentials V_1 and V_2 can be written as

$$\begin{cases} V_1=E_0 \exp[-(\rho-\rho_0/a)^2]\exp[-(z/z_0)] & \rho>\rho_0 \\ V_1=E_0 \exp[-(z/z_0)] & \rho\leqslant\rho_0 \end{cases}, \tag{10}$$

with $\rho=(x^2+y^2)^{1/2}$, and

$$V_2=E_0 \exp[-(x/x_0)^2-(y/y_0)^2]\exp[-(z/z_0)]. \tag{11}$$

x, y, and z correspond to the components of the vector between N and Ar.

TABLE I. Values of the different parameters necessary to build up the full potential energy surface. The first two groups are the Lennard-Jones parameters of the pairwise atom–atom interactions. The last two groups correspond to two alternative descriptions of the interaction of Ar with the lone pair electrons of nitrogen [see Eqs. (12) and (13) in the text].

	S_0	S_1
ϵ_{C-Ar} (cm^{-1})	40.00	46.00
ϵ_{H-Ar} (cm^{-1})	33.00	37.50
ϵ_{N-Ar} (cm^{-1})	55.00	46.00
σ_{C-Ar} (Å)	3.42	3.37
σ_{H-Ar} (Å)	3.21	3.20
σ_{N-Ar} (Å)	3.28	3.28
E_0 (cm^{-1})	570.00	
x_0 (Å)	0.85	
y_0 (Å)	1.47	
z_0 (Å)	4.00	
E_0 (cm^{-1})	570.00	
a (Å)	0.77	
ρ_0 (Å)	0.50	
z_0 (Å)	4.00	

Note that this interaction (between N and Ar) is not isotropic, in order to account for the anisotropy of the lone pair of nitrogen; it depends on the position of the argon relative to the electronic cloud of the N atom. The main difference between V_1 and V_2 is that the V_1 potential is of cylindrical symmetry while V_2 has an ellipsoidal shape. All the parameters used in this work are summarized in Table I.

In this theoretical work, as seen in Sec. II, the aniline molecule was considered to be frozen. However, the geometries are slightly different for the two electronic states. Structures have been evaluated from the work of Christoffersen *et al.*:[36] Aniline is planar in the S_1 state, while the plane of the two N–H bonds in the amino group makes an angle of 43° with respect to the plane of the molecule in the S_0 state. All the details have been previously reported by Hermine *et al.*[10]

Before giving the results of the calculations, we want to mention the experimental observables to which the results are to be compared, in particular in order to adjust the potential parameters for the S_1 surface. These data are the values of the vdW frequencies in S_1, and the electronic $S_1 \leftarrow S_0$ spectral shifts for both the *ring* site and the *nitrogen* site. In the latter case the theoretical value cannot be readily obtained from the present calculations. Indeed we separately performed[37] the calculations of the electronic shift in the (2/1) and (3/0) clusters using MD and the semiclassical spectral density method proposed by Fried and Mukamel.[38] In addition, the parametrization takes into account the TPA–Ar data[20] under the assumption that the same additional N–Ar interaction, evaluated at the equilibrium position (see above), is responsible for the observed blue shift. Some additional information about the recovery of the *ring* site shift is given at the end of Sec. IV.

IV. RESULTS AND DISCUSSION

In this section, we will present results for the S_0 state and the S_1 state. We will discuss the effect of the two different additive terms representing an effective interaction between N and Ar in the S_1 state, as outlined in the previous section. After a brief description of S_0 results, the discussion will focus on the S_1 state because accurate experimental results for the van der Waals modes in this electronic state are available.[10,11]

Table II contains the values of the calculated energies of the first ten eigenstates in S_0 and their assignments. The root mean square amplitudes of vibration along the Cartesian coordinates $\Delta X_i = (\langle d_i^2 \rangle - \langle d_i \rangle^2)^{1/2}$ are also given. These parameters are very useful as a quick way to perform assignments of the calculated bound states. The averaged values $\langle d_x \rangle$ and $\langle d_z \rangle$ are also given ($\langle d_y \rangle$ is always equal to zero by symmetry), but their variations are difficult to correlate with the assignments. The visualization of the wave functions provides unambiguous assignments of the lower eigenstates. As an example, the wave function for state number 2 is shown in Fig. 2. This state is clearly associated to one quantum of excitation of the "bending" motion along the x axis. No coupling with other degrees of freedom is apparent. On the other hand, Fig. 3 is a visualization of the wave function of state number 9. In this case, assignment is less obvious. However, analysis of the wave function together with the ΔX_i values allows us to identify

TABLE II. Eigenenergies, rms amplitudes of vibration along each axis (ΔX_i), mean value, $\langle d_i \rangle$ of each coordinate, and assignments of the first 10 bound states for the aniline–Ar complex in its electronic ground state S_0. The energies are relative to the ground vibrational state whose absolute energy is equal to -360.1 cm^{-1}.

State	Energy (cm^{-1})	ΔX (Å)	ΔY (Å)	ΔZ (Å)	$\langle d_x \rangle$ (Å)	$\langle d_z \rangle$ (Å)	V_x	V_y	V_z
1	00.0	0.36	0.36	0.12	0.04	3.51	0	0	0
2	12.6	0.62	0.38	0.12	0.18	3.52	1	0	0
3	22.0	0.38	0.65	0.12	0.15	3.52	0	1	0
4	25.1	0.78	0.39	0.13	0.17	3.52	2	0	0
5	33.3	0.65	0.68	0.13	0.25	3.52	1	1	0
6	36.7	0.70	0.53	0.16	0.10	3.54	3	0	0
7	38.1	0.69	0.61	0.15	0.16	3.54	0	2	0
8	45.1	0.80	0.70	0.13	0.21	3.53	2	1	0
9	46.6	0.50	0.70	0.17	0.26	3.55	0	0	1
10	49.3	1.00	0.44	0.15	0.07	3.54	4	0	0

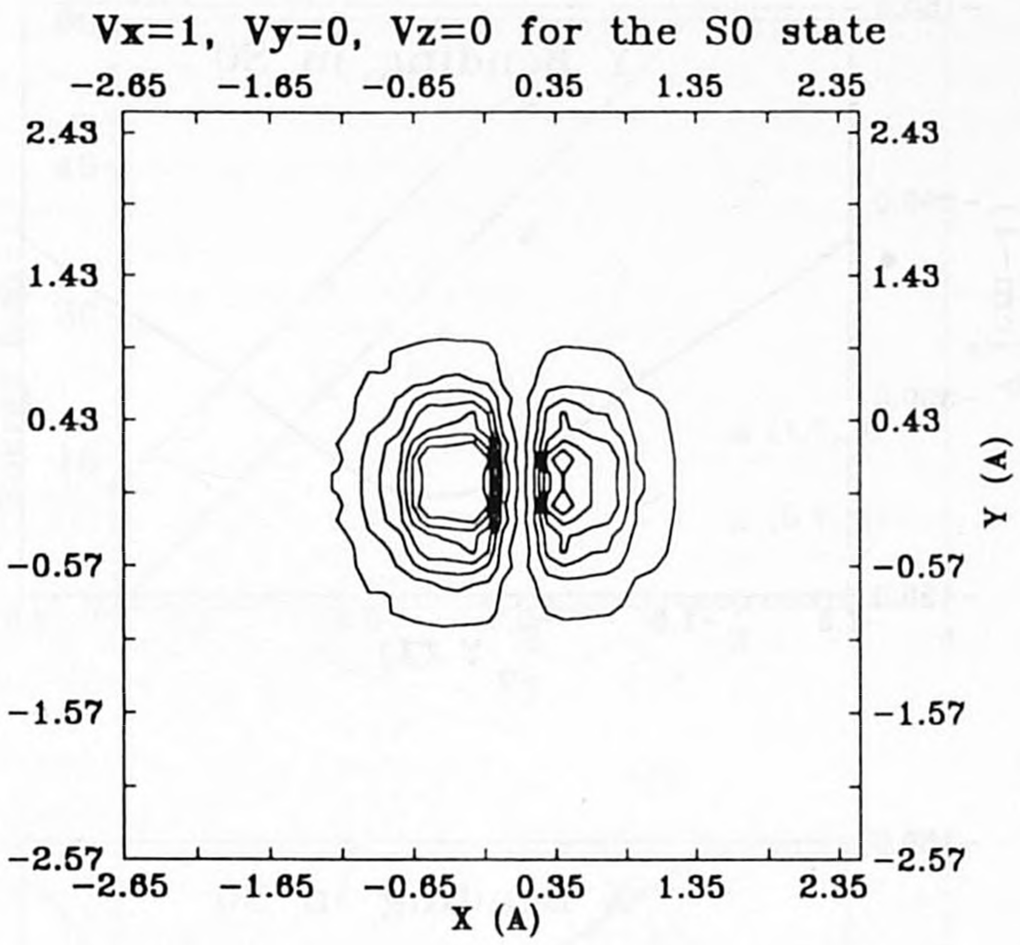

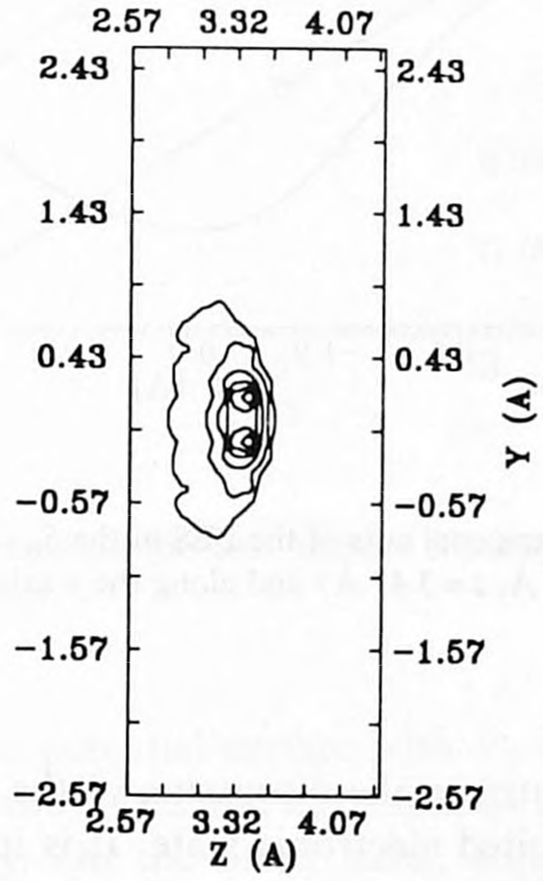

FIG. 2. Contour plots of the state number 2 in S_0 (bending along the x axis, b_x^1). The top panel corresponds to the cut at $z=3.50$ Å, the bottom panel to the cut at $x=-0.08$ Å.

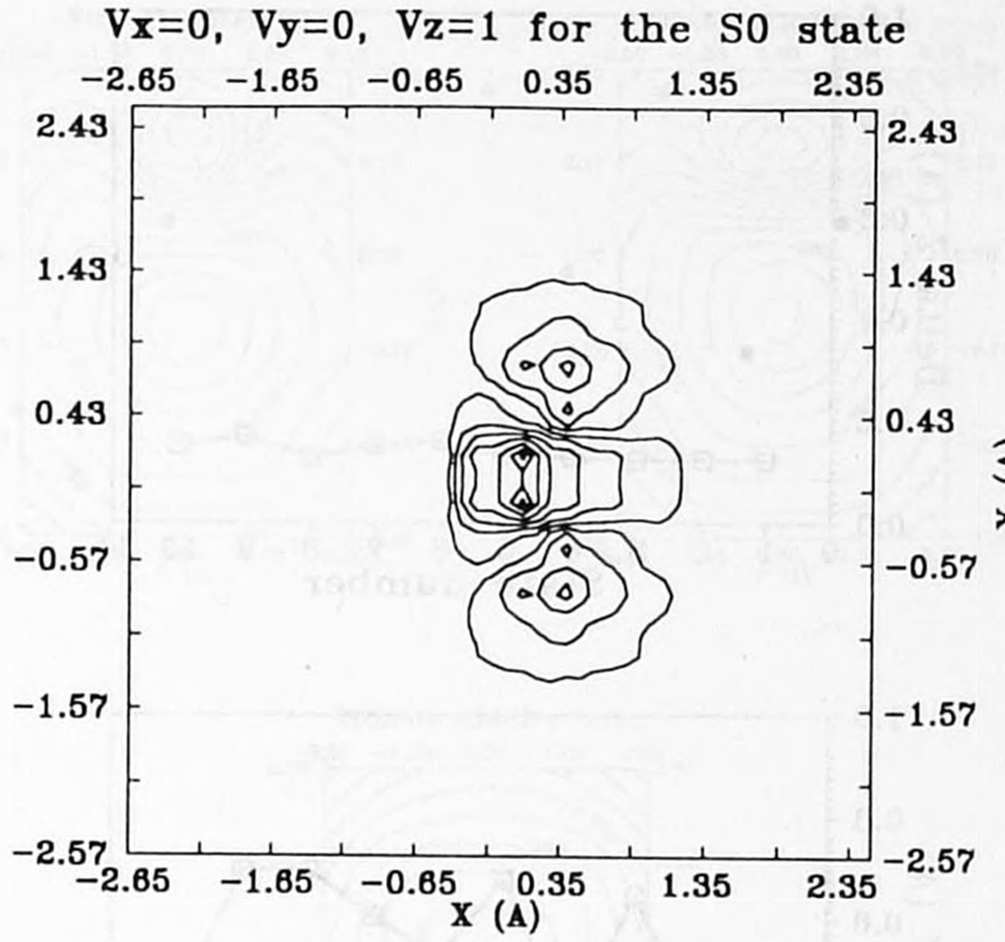

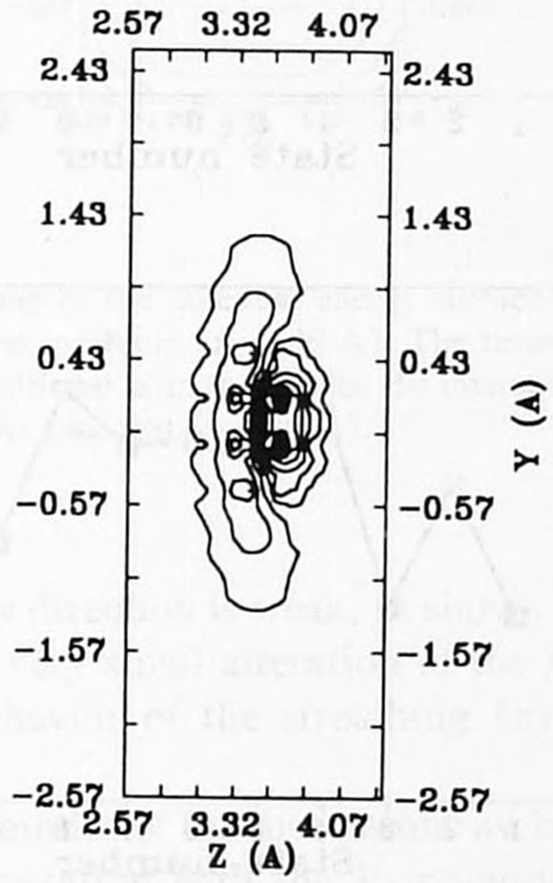

FIG. 3. Contour plots of the state number 9 in S_0 (stretching along the z axis s_z^1). The top panel corresponds to the cut at $z=3.50$ Å, the bottom panel to the cut at $x=-0.08$ Å.

this state as the stretching mode (motion along the z axis). We note however that in this state a strong coupling with the motion along the y axis is involved, as apparent from both the wave function and in the ΔX_i values [the increase of ΔX_3 (or ΔZ) is accompanied by an increase of ΔX_2 (or ΔY)]. It is most probably a linear combination of ($V_x=0, V_y=0, V_z=1$) and ($V_x=0, V_y=2, V_z=0$).

Analysis of the ΔX_i values shown in Fig. 4 also gives information on the dynamical behavior of the Ar atom. The ΔZ value reflects the amplitude of the motion along the z axis (perpendicular to the plane of aniline). From Fig. 4, this value is small in comparison with the ΔX and ΔY values. The aromatic molecule really acts as a microsurface for the Ar atom. Motion in a plane parallel to the chromophore is easier than in the direction perpendicular to the aromatic plane. Moreover, the ΔX and ΔY values are quite large in absolute magnitude, reaching a significant fraction of a C–C bond length. Comparison between ΔX and ΔY in Fig. 4 also reveals that motions along the x and y axes are of the same order of magnitude. From the oscillations, the states corresponding to pure b_x, pure b_y, or combinations b_x plus b_y are also clearly identified. States number 6 and number 7 indeed involve anharmonic coupling between b_x and b_y motions.

In the S_0 state, the three calculated fundamental frequencies are $\nu_x=12.6$, $\nu_y=22.0$, $\nu_z=46.6$ cm^{-1}, where ν_x and ν_y correspond to the bending motions along the x and y axes, respectively, and ν_z to the stretching frequency (in a direction perpendicular to the aromatic plane). Figure 5 shows the one-dimensional potential curves in S_0 as a function of x and y, respectively (the other coordinates being fixed at their equilibrium value). These two curves are very

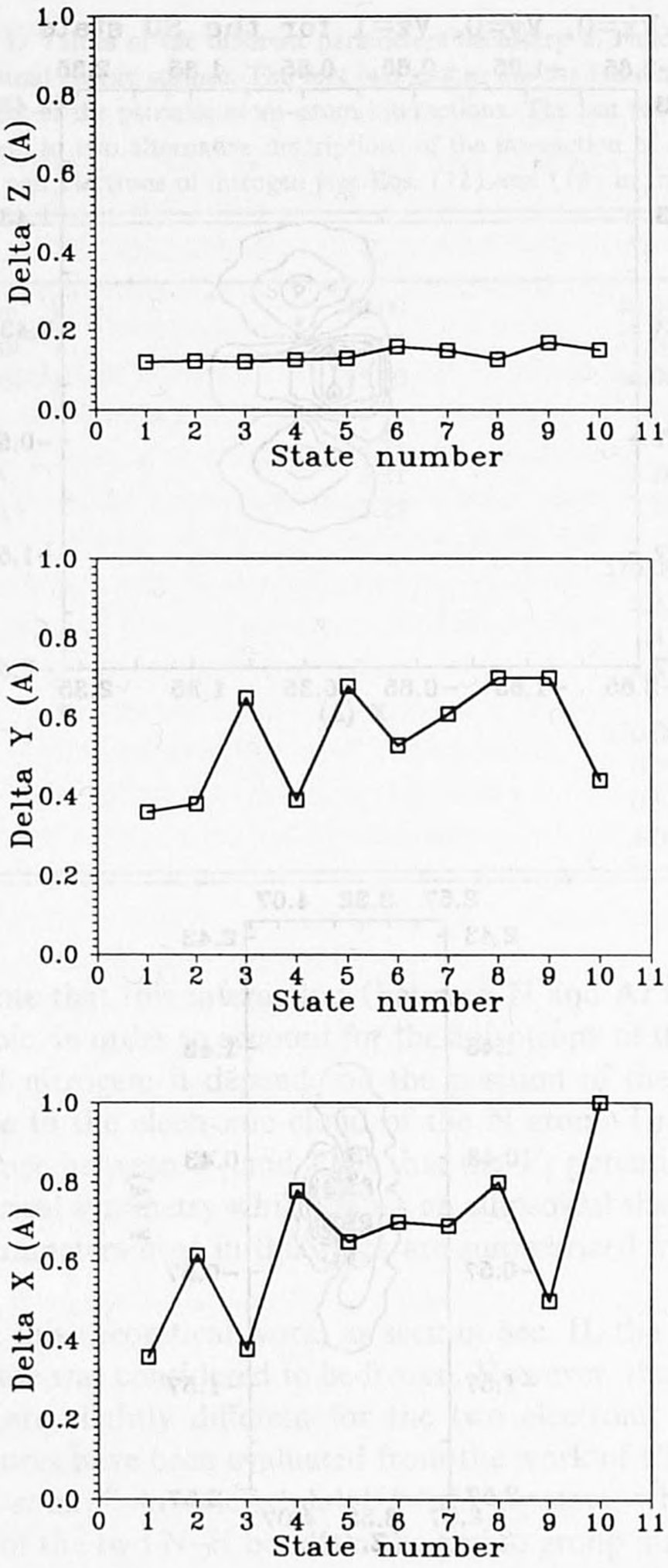

FIG. 4. Root-mean-square amplitudes of vibration in each direction, Δx, Δy, and Δz for the first ten vibrational eigenstates in S_0.

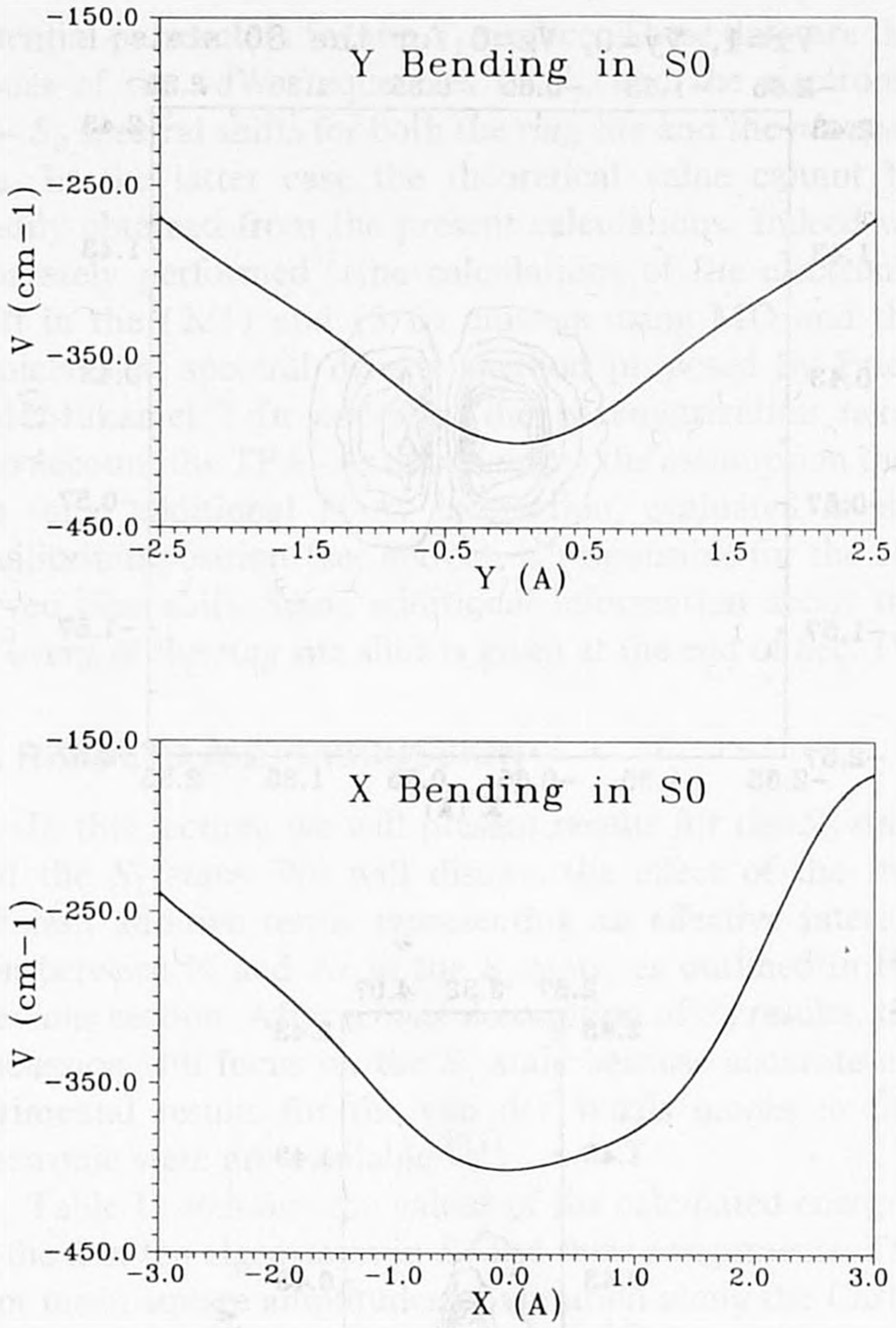

FIG. 5. One-dimensional cuts of the PES in the S_0 state along the x axis (bottom, $y=0.00$ Å, $z=3.47$ Å) and along the y axis (top, $x=-0.08$ Å, $z=3.47$ Å).

different. In particular the x bending curve presents a net asymmetry due to the interaction between Ar and the two out of plane hydrogen atoms, while the y bending curve is symmetric.

As is visible at the bottom of Fig. 6, the progression in the bending mode along the x axis appears quite harmonic. $\Delta\nu_x$ is equal to 12.6 and 12.5 cm^{-1} ($\Delta\nu_x$ being the difference between two successive bending x modes). With one quantum of excitation in the motion along the y axis, these values are reduced as apparent from the slopes on the straight lines. On the other hand, the y bending motion behaves differently (top of Fig. 6). $\Delta\nu_y$ is equal to 22.0 and 16.1 cm^{-1}. As we saw before with the corresponding wave function, b_y^2 is strongly coupled with the stretching mode s_z^1 ($\nu_z=46.6$ cm^{-1}). This coupling tends to push away the two corresponding states (Fermi resonance). It corresponds to a "decrease" of the b_y^2 frequency and an "increase" of the s_z^1 frequency.

We now turn to the discussion of the results obtained in the first excited electronic state. It is important first to consider the differences between the three PES (potential energy surface) without the additive term and with the two different additive potentials V_1 and V_2 defined by Eqs. (10) and (11) in Sec. II. Figure 7 displays the contours of the three PES (in the first electronic state S_1) in a plane parallel to the aniline molecule at the distance $z=+3.39$ Å of this plane, i.e., nearly containing the principal minimum (above the center of the ring). The values of the frequencies are mainly related to the shape of the potential surface in this region. It can be seen from this figure that the surfaces present important differences. First of all, note that the PES is significantly affected by the addition of the V_1 potential. In particular, V_1 strongly perturbs the region near the absolute minimum of the potential (above the center of the aromatic ring). For each of these three PES the Hamiltonian is solved in the same way as for the S_0 state. Table III contains the values of the energies of the first 15 eigenstates and their assignments when using the V_2 term. In Table IV, the derived sets of vdW frequencies are reported for a comparison of the three surfaces in the S_1 state. The x bending is clearly very sensitive to the addition of a "blue" potential, its frequency being maximum when the V_1 potential is added. As is apparent in

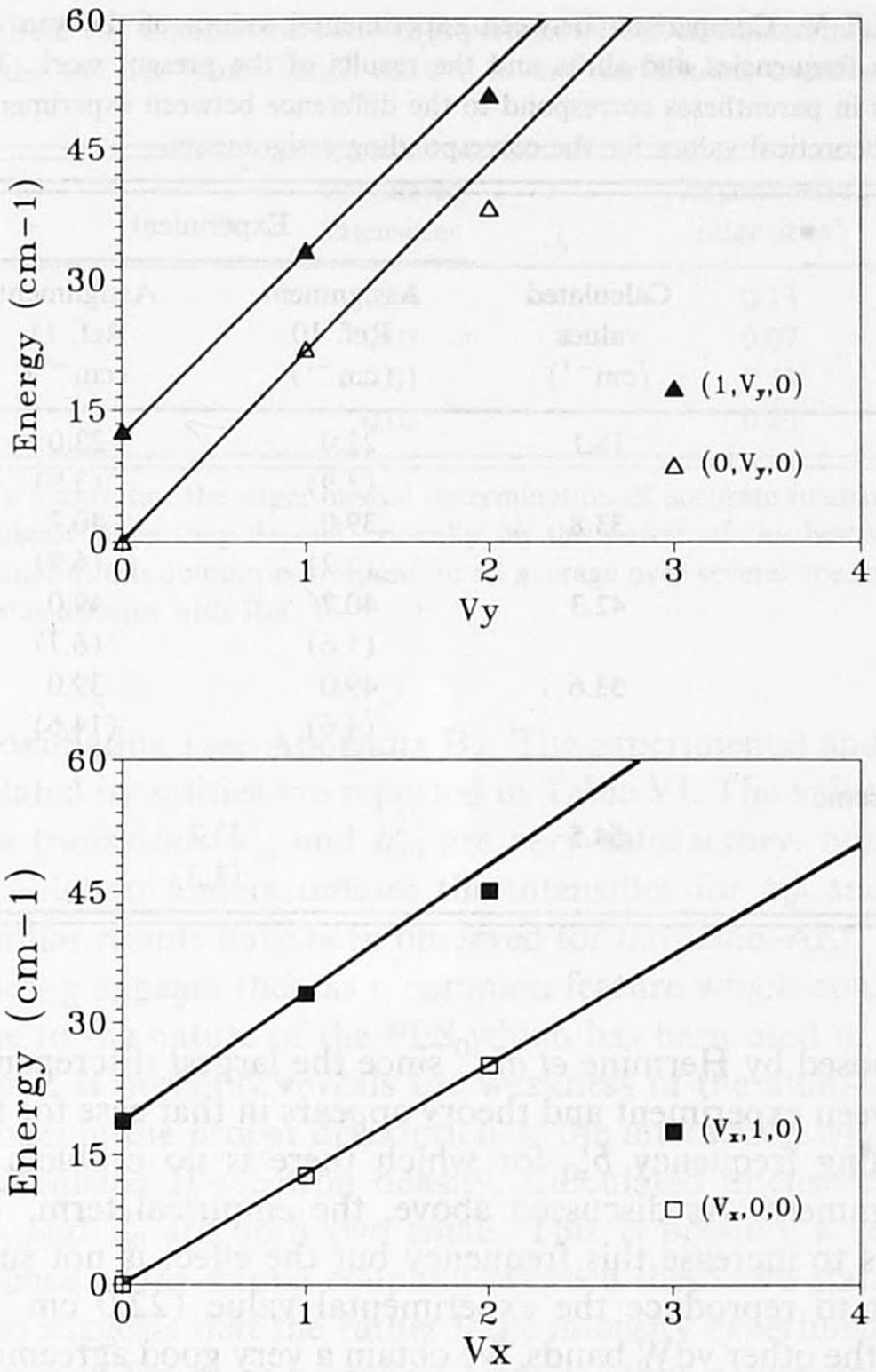

FIG. 6. Plots of the eigenenergies as a function of the b_x and b_y quantum numbers in the S_0 state.

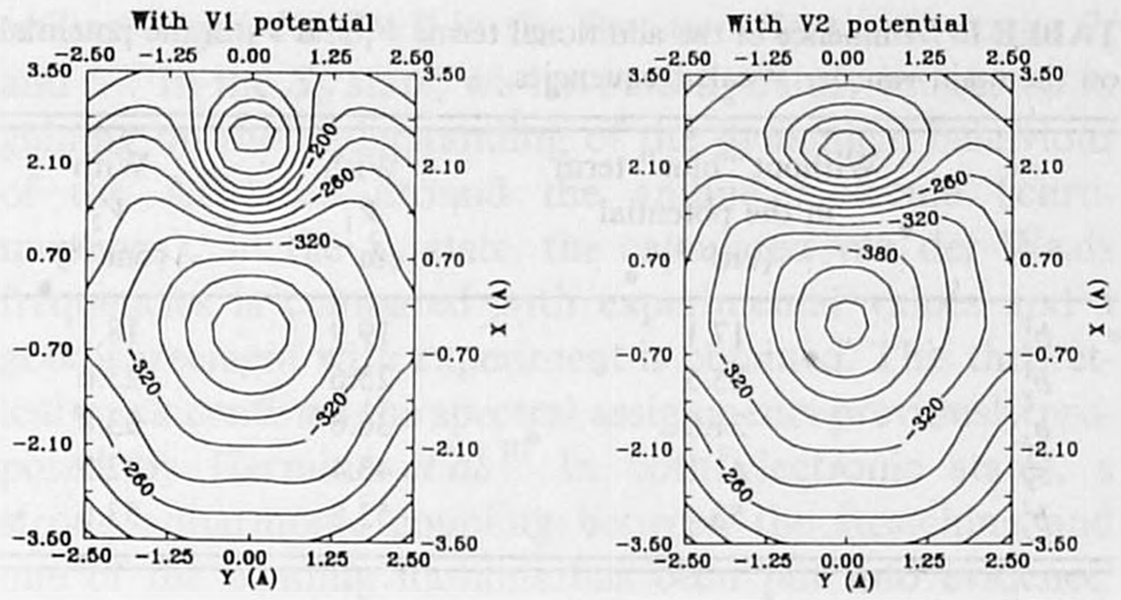

FIG. 7. Contour map of the potential energy surface in S_1 in a plane parallel to the aniline molecule ($z=3.39$ Å). The three panels differ by the choice of the additional term to describe the interaction of the Nitrogen lone pair with Ar (see text for details).

Figs. 7 and 8, the potential surface with V_2 is significantly perturbed along the x axis and this explains the increase of the b_x frequency. On the other hand, addition of these empirical terms has almost no effect on the value of the y bending frequencies. Indeed, the perturbation of the total potential in the y direction is weak, as shown in Fig. 7, and this results in a very small alteration of the y bending frequency. The behavior of the stretching (z) frequency is intermediate.

For the remainder of the discussion, we have chosen to use the parametrization with the V_2 potential (whose results are contained in the Table III), because the V_1 po-

TABLE III. Eigenenergies, rms amplitudes of vibration along each axis (ΔX_i), mean value, $\langle d_i \rangle$ of each coordinate, and assignments of the first 15 bound states for the aniline–Ar complex in its S_1 electronic excited state. The energies are relative to the ground vibrational state whose absolute energy is equal to -405.6 cm^{-1}.

State	Energy (cm^{-1})	ΔX (Å)	ΔY (Å)	ΔZ (Å)	$\langle d_x \rangle$ (Å)	$\langle d_z \rangle$ (Å)	V_x	V_y	V_z
1	00.0	0.30	0.32	0.12	−0.23	3.44	0	0	0
2	18.1	0.53	0.33	0.12	−0.18	3.45	1	0	0
3	25.6	0.32	0.58	0.12	−0.19	3.45	0	1	0
4	33.8	0.65	0.37	0.14	−0.21	3.46	2	0	0
5	42.2	0.55	0.60	0.12	−0.13	3.46	1	1	0
6	42.3	0.40	0.55	0.16	−0.19	3.48	0	0	1
7	49.7	0.79	0.42	0.14	−0.21	3.48	3	0	0
8	53.6	0.36	0.64	0.16	−0.18	3.49	0	2	0
9	56.3	0.64	0.68	0.14	−0.18	3.48	2	1	0
10	61.0	0.63	0.64	0.15	−0.16	3.49	1	0	1
11	62.6	0.47	0.79	0.15	−0.15	3.49	0	1	1
12	65.0	0.90	0.46	0.16	−0.33	3.49	4	0	0
13	70.2	0.61	0.59	0.17	−0.12	3.50	2	0	1
14	70.6	0.79	0.72	0.14	−0.18	3.48	3	1	0
15	74.5	0.62	0.79	0.17	−0.24	3.50	1	2	0

TABLE IV. Influence of the additional terms V_1 and V_2 in the potential on the main van der Waals frequencies.

	Without "blue" term in the potential (cm^{-1})	With V_1 (cm^{-1})	With V_2 (cm^{-1})
b_x^1	17.1	19.9	18.1
b_y^1	25.5	25.6	25.6
b_x^2	31.0	36.6	33.8
s_z^1	41.1	43.4	42.3
b_y^2	53.4	53.5	53.6

tential could not reproduce the blue contribution of $+35$ cm^{-1} (when the Ar atom takes its place in a "nitrogen" site) in the semiclassical simulations.[37] Since we want to use this potential to investigate the spectra of higher clusters, this choice appeared to be most suitable for the reproduction of the experimental shifts and frequencies by spectral density methods.[37,38]

Table V compares the experimental and theoretical results. For the vdW vibrations in the S_1 state, two different assignments have been proposed by Hermine *et al.*[10] and Bieske *et al.*[11] They are in agreement about the b_{x0}^1 frequency, but they differ concerning the other features (b_{x0}^2, b_{y0}^2 and s_{z0}^1). The present results confirm the assignments

TABLE V. Comparison between experimental values of the van der Waals frequencies and shifts and the results of the present work. The values in parentheses correspond to the difference between experimental and theoretical values for the corresponding assignments.

		Experiment	
	Calculated values (cm^{-1})	Assignment Ref. 10 (cm^{-1})	Assignment Ref. 11 (cm^{-1})
b_{x0}^1	18.1	22.0 (3.9)	22.0 (3.9)
b_{x0}^2	33.8	39.0 (5.2)	40.7 (6.9)
s_{z0}^1	42.3	40.7 (1.6)	49.0 (6.7)
b_{y0}^2	53.6	49.0 (4.6)	39.0 (14.6)
Electronic shift	54.5	53.2 (1.3)	

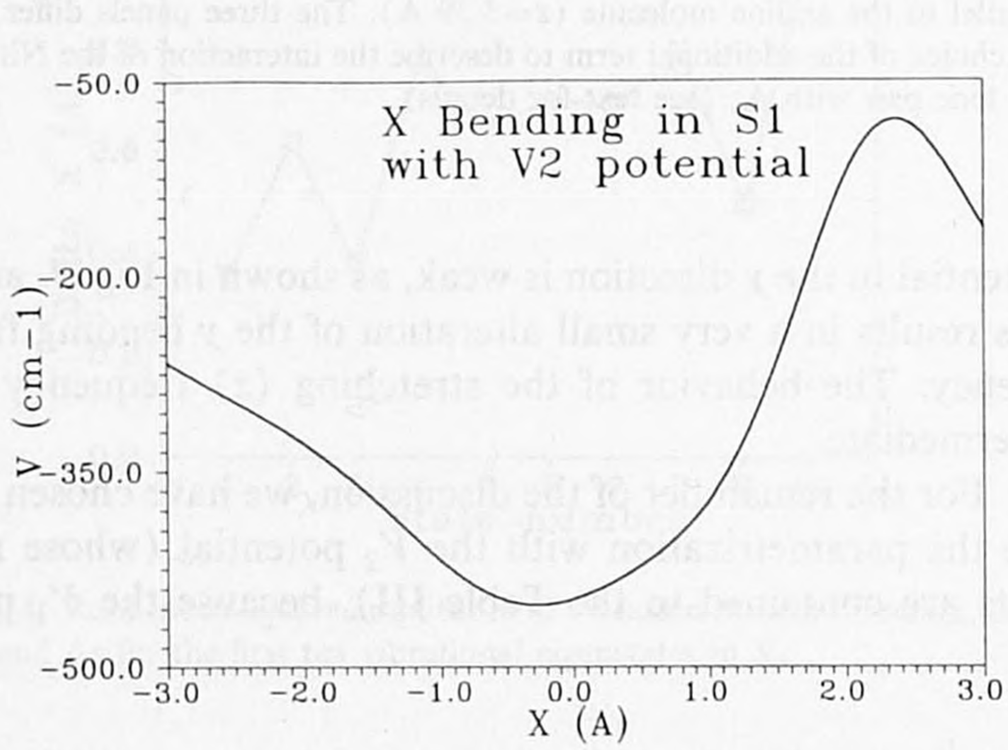

FIG. 8. One-dimensional cuts of the PES in the S_1 state along the x axis ($y=0.00$ Å, $z=3.39$ Å) with the additional V_2 term in the surface (top) or without it (bottom).

proposed by Hermine *et al.*[10] since the largest discrepancy between experiment and theory appears in that case for the bending frequency b_{x0}^1 for which there is no problem of assignment. As discussed above, the empirical term, V_2, tends to increase this frequency but the effect is not sufficient to reproduce the experimental value (22.0 cm^{-1}). For the other vdW bands, we obtain a very good agreement with experiment when we use the assignments proposed by Hermine *et al.*[10] It is interesting to note that the apparent stretching frequency s_{z0}^1 in the S_1 state is smaller than in the S_0 state (42.3 cm^{-1} instead of 46.6 cm^{-1}). This surprising result is due to a Fermi resonance with the b_y^2 level. As discussed above, in the S_0 state, the s_z^1 level is pushed towards higher energies because of its coupling with the lower b_y^2 level. In the S_1 state the situation is reversed: b_y^2 is higher in energy than s_z^1 so that the apparent stretching frequency is lowered.

Also given in Table V is the value of the electronic spectral shift. It is important to note that the theoretical value of this shift takes into account the change ($\cong 9$ cm^{-1}) in the zero-point energy of the aniline inversion motion induced by the presence of the Argon atom. This correction is made necessary by the following facts: (i) The model surfaces discussed above involve the aniline molecule in frozen geometries which differ in the two electronic states S_0 and S_1 mainly by the equilibrium value of the inversion coordinate Q: $Q=0$ in S, $Q=Q$ (43° angle) in S. (ii) The inversion frequency (40 cm^{-1}) has the same order of magnitude as the vdW vibrations. (iii) A one-dimensional quantum mechanical treatment of the inversion motion (described in Appendix A) reveals that it is perturbed by the presence of the argon atom in the complex but not blocked. The method used to evaluate the electronic spectral shift is given in Appendix A.

We have also calculated the intensities of the vibronic transitions between the ground vibrational state (in S_0) and the vdW vibrational states in the S_1 state. These calculations have been performed in the Franck–Condon ap-

TABLE VI. Comparison between experimental and calculated intensities of the van der Waals bands relative to the vibrationless transition (0_0^0 band).

	Calculated intensities	Experimental intensities[a]
b_{x0}^1	0.14	0.13
b_{x0}^2	0.08	0.07
s_{z0}^1	0.01	0.33
b_{y0}^2	0.03	0.20

[a]We found that the experimental determination of accurate intensities is difficult since they depend critically on the power of the lasers. The values in this column correspond to an average over several spectra and are consistent with Ref. 11.

proximation (see Appendix B). The experimental and calculated intensities are reported in Table VI. The values for the transitions b_{x0}^1 and b_{x0}^2 are very satisfactory, but this calculation underestimates the intensities for b_{y0}^2 and s_{z0}^1. Similar results have been observed for tetrazine–Ar.[29] This finding appears then as a common feature which could be due to the nature of the PES which has been used in both cases. It probably reveals the weakness of the atom–atom model in the proper description of the interaction with the delocalized Π–electron density. Calculated intensities for b_{y0}^2 and s_{z0}^1 are both two small. This is possibly a consequence of the strong coupling between these two states. It also suggests that the rather large intensity experimentally observed for b_{y0}^2 is borrowed from s_{z0}^1, thus confirming the existence of this coupling.

As we noted in Sec. II, all the calculations have been performed for $\mathbf{J}=\mathbf{0}$. For comparison with experimental spectra taken at rotational resolution it is interesting to look at the rotational constants. In this last part, theoretical rotational constants have been evaluated in the two electronic states by considering the Hamiltonian H_{rovib} [Eq. (8)] as a perturbation of H_{eff}. The method used (van Vleck perturbation theory) has been extensively described by Brocks *et al.*[28] Comparison between our theoretical results and experimental results obtained by Yamanouchi *et al.*[18] are shown in Table VII. The overall agreement is very good.

IV. CONCLUSION

We have reported fully quantum mechanical calculations of vibrational states of the van der Waals system aniline–argon for $\mathbf{J}=\mathbf{0}$ in the first two electronic states S_0 and S_1. In the S_0 state, we have been mainly interested in gaining on the understanding of the dynamical behaviour of the Ar atom around the aniline molecule (chromophore). In the S_1 state, the calculated van der Waals frequencies is compared with experimental values and a good agreement with experiment is obtained. This theoretical work confirms the spectral assignments previously proposed by Hermine *et al.*[10] In both electronic states, a strong anharmonic coupling between the stretching and one of the bending motions has been put into evidence. Moreover, the influence of an empirical anisotropic term in the S_1 state potential (between the Ar atom and the N atom) has been studied and discussed. This potential has been added to the original atom–atom potential in order to reproduce experimental blue shifts which are observed in larger clusters when one Ar atom occupies a binding site located near the $-NH_2$ functional group.[10] This *positive* term accounts for the reduction of the attraction between the nitrogen atom and the argon atom (responsible for the observed blue shift). Not only does it improve the quality of the agreement with experimental data for the 1:1 complex, but it succeeds in the semiclassical spectra simulations of large clusters.[37]

The rotational constants have also been calculated and their values are very close to the experimental ones given by Yamanouchi *et al.*[18]

In the Franck–Condon approximation, the intensities of the bands in the electronic spectrum between S_0 and S_1 have been evaluated. Intensities for the b_{y0}^2 and the s_{z0}^1 transitions are largely underestimated.

The major conclusion of this work is that a relatively simple potential energy surface, obtained without extensive *ab initio* calculations, is able to reproduce satisfactorily most of the important observables (frequencies, geometries,...) in this simple cluster which can be considered as a prototype of a large class of aromatic-rare gases solvent microclusters. Due to the good knowledge of the rare gas-rare gas interaction and to the weakness of the three body forces, it is thus possible to extend the theoretical investigations to clusters of large size[37] or to related solute/solvent systems.

TABLE VII. Comparison between experimental (Ref. 18) and theoretical values of the rotational constants for the vibrational ground state in both S_0 and S_1 electronic states.

Rotational constants in the ground vibrational state	S_0		S_1	
	Calc. (cm^{-1})	Expt.[a] (cm^{-1})	Calc. (cm^{-1})	Expt.[a] (cm^{-1})
A	0.0587	0.0594	0.0585	0.0592
B	0.0388	0.0399	0.0394	0.0409
C	0.0313	0.0321	0.0324	0.0332

[a]Reference 18.

APPENDIX A: EVALUATION OF THE $S_1 \leftarrow S_0$ SPECTRAL SHIFT

In the free ground state (S_0) aniline molecule, the inversion motion undergoes the quantum mechanical tunnelling characteristic of the symmetrical double-well intramolecular potential, which has been shown[39] to be well described by the function

$$U_0(Q_I)=A+BQ_I^2+CQ_I^4 \tag{A1}$$

with $A=547.00$, $B=-1942.24$, and $C=1724.09\ cm^{-1}$.

In this expression of the intramolecular potential of free aniline, the normal coordinate associated to the inversion mode Q_I can be approximated as the angle (expressed in radian) between the aromatic plane and the $-NH_2$ plane.

The vdW intermolecular interaction can be constructed (as above) as a sum of pairwise atom–atom terms for different geometries of the aniline subunit. Thus the resulting vdW interaction V has a **weak**, parametric, dependence on the inversion coordinate

$$V=V(\mathbf{d};Q_I).$$

Solving the Schrödinger equation for the vdW motion **d** for given values of Q_I (frozen geometries) leads to the energies of the ground state level as a function of Q_I, i.e., $D_0(Q_I)$. The Q_I dependence is small enough to be linearized as

$$D_0(Q_I)=D_0(0)+\lambda Q_I\,, \tag{A2}$$

where

$$\lambda=[\,D_0(Q_0)-D_0(-Q_0)\,]/2Q_0 \tag{A3}$$

can be approximated as

$$\lambda=[\,D_e(Q_0)-D_e(-Q_0)\,]/2Q_0\,. \tag{A4}$$

Numerical evaluation with the atom–atom parameters of Table I gives $\lambda Q_0=10\ \mathrm{cm}^{-1}$ (the binding energy D_e of the Ar atom has been calculated for the two inequivalent structures $Q_I=+Q_0$ and $-Q_0$).

The total potential for the vibrations in the complex is the sum of intramolecular and vdW interactions. The intramolecular modes different from inversion are discarded because they are essentially unaffected by the presence of the Ar atom. Thus

$$V_{\text{total}}=U_0(Q_I)+V(\mathbf{d};Q_I). \tag{A5}$$

Although the inversion and vdW motion should normally be solved simultaneously, they can be separated following the above approximate linearization procedure:

$$\begin{aligned}V_{\text{total}}&=U_0(Q_I)+V(\mathbf{d};Q=0)+\lambda Q_I\\&=U_0(Q_I)+V(d;Q_0)+\lambda Q_I-\lambda Q_0\,,\end{aligned} \tag{A6}$$

where $V(\mathbf{d};Q_0)$ is the frozen geometry vdW potential used in the body of this article. The order of magnitude of λQ_I is such that it can be considered as a perturbation of the free molecule inversion potential in the new inversion potential within the complex

$$U(Q_I)=U_0(Q_I)+\lambda Q_I \tag{A7}$$

with

$$V_{\text{total}}=U(Q_I)+V(\mathbf{d};Q_0)-\lambda Q_0\,. \tag{A8}$$

This results in a one-dimensional treatment of the inversion motion in a nonsymmetrical double well, with substantial computational savings. The problem has been solved numerically. The ground state wave function is asymmetrical but clearly shows that the inversion is not blocked. Thus although the two potential minima are shifted in energy, respectively, to higher and lower values, the eigenenergy of the ground state is almost unchanged (about 1 cm^{-1}) (although it is not the case for the zero-point energy).

Then the ground state energy of the complex in S_0 is

$$E_0''=(E_0'')^{\text{free}}+D_0''(Q_0)-\lambda Q_0\,, \tag{A9}$$

where $(E_0'')^{\text{free}}$ is the ground state energy in free S_0 aniline.

Assuming that the ground vibrational state energy for the complex in S_1 (frozen geometry $Q_I=0$) is a simple sum of intramolecular and vdW terms:

$$E_0'=(E_0')^{\text{free}}+D_0'(0) \tag{A10}$$

the spectral shift of the $S_1\leftarrow S_0$ electronic transition in the vdW complex relative to the free molecule then follows:

$$\begin{aligned}\Delta E&=[\,(E_0')^{\text{free}}+D_0'(0)\,]-[\,(E_0'')^{\text{free}}+D_0''(Q_0)-\lambda Q_0]\\&\quad-[\,(E_0')^{\text{free}}-(E_0'')^{\text{free}}]\end{aligned} \tag{A11}$$

$$\begin{aligned}&=D_0'(0)-D_0''(Q_0)+\tfrac{1}{2}[\,D_e(Q_0)-D_e(-Q_0)\,],\end{aligned} \tag{A12}$$

where use has been made of Eq. (A4).

APPENDIX B: CALCULATION OF THE FRANCK–CONDON FACTORS

The intensity of a vibronic transition is proportional to

$$\begin{aligned}I_{0n}&=|\,\langle\phi_0(\mathbf{d})\phi_{\text{ev}}^{(0)}|\,\vec{\mu}\cdot\vec{e}\,|\,\phi_n(\mathbf{d})\phi_{\text{ev}}^{(1)}\rangle\,|^2\\&=|\,\langle\phi_0(\mathbf{d})\,|\mu_{01}|\,\phi_n(\mathbf{d})\rangle\,|^2\end{aligned}$$

with

$$\mu_{01}=|\,\langle\phi_{\text{ev}}^{(0)}|\,\vec{\mu}\cdot\vec{e}\,|\,\phi_{\text{ev}}^{(1)}\rangle\,|^2$$

and with $\phi_0(\mathbf{d})$ and $\phi_n(\mathbf{d})$ being the van der Waals vibrational wave functions in the ground and first excited state, respectively, while $\phi_{\text{ev}}^{(0)}$ and $\phi_{\text{ev}}^{(1)}$ are the vibronic wave functions of aniline in the S_0 and S_1 state, respectively.

Finally, $\vec{\mu}$ is the dipole operator and μ_{01} is the electronic transition dipole moment.

In the Franck–Condon approximation, we suppose that μ_{01} does not depend on **d**. In this case, I_{0n} is proportional to $|\,\langle\phi_0|\phi_n\rangle\,|^2$

In our calculations, we took the same values of $\mathbf{d}^e$ and the same basis set (with the same parameters ω_x, ω_y, ω_z) in the two electronic states. Then, $|\,\langle\phi_0|\phi_n\rangle\,|^2$ will be just equal to

$$|\,\langle\phi_0|\phi_n\rangle\,|^2=\sum_{k,l,m}C_{k,l,m}^{(0)}C_{k,l,m}^{(n)}.$$

[1] A. Amirav, U. Even, and J. Jortner, Chem. Phys. Lett. **72**, 16 (1980).
[2] U. Even, N. Ben-Horin, and J. Jortner, Phys. Rev. Lett. **62**, 140 (1989).
[3] S. Leutwyler and J. Boesiger, Chem. Rev. **90**, 489 (1990).
[4] T. Troxler and S. Leutwyler, J. Chem. Phys. **95**, 4010 (1991).
[5] M. Schmidt, M. Mons, and J. le Calve, Chem. Phys. Lett. **177**, 371 (1991).
[6] U. Even, A. Amirav, S. Leutwyler, M. J. Ondrechen, Z. Berkovitch-Yellin, and J. Jortner, Faraday Discuss. Chem. Soc. **73**, 153 (1982).
[7] K. Rademann, B. Brutschy, and H. Baumgartel, Chem. Phys. **80**, 129 (1983).
[8] M. I. Shchuka, A. L. Motyka, and M. R. Topp, Chem. Phys. Lett. **164**, 87 (1989).
[9] P. D. Dao, S. Morgan, and A. W. Castelman, Jr., Chem. Phys. Lett. **111**, 38 (1984).
[10] P. Hermine, P. Parneix, B. Coutant, F. G. Amar, and Ph. Bréchignac, Z. Phys. D **22**, 529 (1992).

[11] E. J. Bieske, A. S Uichanco, M. W. Rainbird, and A. E. W. Knight, J. Chem. Phys. **94**, 7029 (1991).
[12] S. Douin, P. Parneix, and Ph. Bréchignac, Z. Phys. D **21**, 343 (1991).
[13] P. D. Dao, S. Morgan, and A. W. Castleman, Jr., Chem. Phys. Lett. **113**, 219 (1985).
[14] T. Troxler, R. Knochenmuss, and S. Leutwyler, Chem. Phys. Lett. **159**, 554 (1989).
[15] T. Kobayashi, K. Homna, O. Kajimoto, and S. Tsuchiya, J. Chem. Phys. **86**, 1111 (1987).
[16] Y. D. Park and D. H. Levy, J. Chem. Phys. **81**, 5527 (1984).
[17] T. Weber and H. J. Neusser, J. Chem. Phys. **94**, 7689 (1991).
[18] K. Yamanouchi, S. Isogai, S. Tsuchiya, and K. Kuchitsu, Chem. Phys. **116**, 123 (1987).
[19] M. Schmidt, M. Mons, J. Le Calvé, P. Millié, and C. Cossart-Magos, Chem. Phys. Lett. **183**, 69 (1991).
[20] G. Meijer, G. Berden, W. L. Meerts, H. E. Hunziker, M. S. De Vries, and H. R. Wendt, Chem. Phys. **163**, 209 (1992).
[21] D. Bahatt, U. Even, and J. Jortner, Chem. Phys. Lett. **117**, 527 (1985).
[22] M. L. Sage and J. Jortner, J. Chem. Phys. **82**, 5437 (1985).
[23] M. R. Nimlos, M. A. Young, E. R. Bernstein, and D. F. Kelley, J. Chem. Phys. **91**, 5268 (1989).
[24] J. J. F. Ramaekers, H. K. Van Dijk, J. Langelaar, and R. P. H. Rettschnick, Faraday Discuss. Chem. Soc. **75**, 183 (1983).
[25] E. A. Outhouse, G. A. Bickel, D. R. Demmer, and S. C. Wallace, J. Chem. Phys. **95**, 6261 (1991).
[26] J. A. Beswick and J. Jortner, Adv. Chem. Phys. **47**, 363 (1981).
[27] G. Brocks and T. Huygen, J. Chem. Phys. **85**, 3411 (1986).
[28] G. Brocks and D. Van Koeven, Mol. Phys. **63**, 999 (1988).
[29] A. R. Tiller and D. C. Clary, J. Chem. Phys. **92**, 5875 (1990).
[30] E. B. Wilson, Jr., J. C. Decius, and P. C. Cross, *Molecular Vibrations* (Dover, New York, 1980), Chap. 2.
[31] J. K. G. Watson, Mol. Phys. **15**, 479 (1968).
[32] A. Messiah, *Quantum Mechanisms* (North-Holland, Amsterdam, 1961), Chap. 10.
[33] M. Abramowitz and I. A. Stegun, *Handbook of Mathematical Functions* (National Bureau of Standards, Gaithersburg, Maryland, 1980), Chap. 2.
[34] J. R. Lombardi, J. Chem. Phys. **50**, 3780 (1969).
[35] M. J. Ondrechen, Z. Berkovitch-Yellin, and J. Jortner, J. Am. Chem. Soc. **103**, 6586 (1981).
[36] J. Christoffersen, J. M. Hollas, and G. H. Kirby, Mol. Phys. **16**, 441 (1969).
[37] P. Parneix and F. G. Amar, Ph. Bréchignac (work in progress).
[38] L. E. Fried and S. Mukamel, Phys. Rev. Lett. **66**, 2340 (1991).
[39] J. M. Hollas, M. R. Howson, T. Ridley, and L. Halonen, Chem. Phys. Lett. **98**, 611 (1983).